journal

J. Am. Ceram. Soc., 86 [7] 1138–45 (2003)

Photocatalytic Activity of Monodispersed Spherical TiO_2 Particles with Different Crystallization Routes

Churl Hee Cho and Do Kyung Kim*

Department of Materials Science and Engineering, Korea Advanced Institute of Science and Technology, 373-1 Kusong-dong, Yusong-gu, Taejon 305-701, Korea

Do Hyeong Kim*

Inorganic Materials Laboratory, Research Institute of Industrial Science and Technology, 32 Hyoja-dong, Pohang 790-330, Korea

Monodispersed spherical TiO_2 particles were prepared by hydrothermal crystallization and/or calcination of spherical amorphous particles, synthesized by thermal hydrolysis of $TiCl_4$. The crystallized spherical particles were secondary agglomerates of primary nanocrystallites. Different crystallization routes and conditions provided the spherical TiO_2 particles with wide particle characteristics, such as the fraction of crystallization, the size and shape of the primary nanocrystallites, and the specific surface area. The photocatalytic activity showed complex dependence on the crystallization routes and conditions. The complex dependence behavior could be explained by combining the effects of the fraction of crystallization, the specific surface area, and the adsorption ability for hydroxyl ions. Especially, in the present study, the hydrothermally crystallized TiO_2 particles with large primary nanocrystallites showed the highest photocatalytic activity. The high photocatalytic activity mainly resulted from the high surface adsorption ability for hydroxyl ions, which was closely related to the well-developed (flat and faceted) morphology of primary nanocrystallite.

I. Introduction

TITANIUM DIOXIDE (TiO_2) particle is a candidate photocatalyst. Photocatalysis is a photon-assisted electrochemical reaction on small semiconductor particles. Since the pioneering work in this field in 1972,[1] nanoparticles have been used as photocatalysts. In the nanoparticle-applied photocatalysis process, one of the drawbacks was the difficulty in handling the nanocatalysts due to their nanometer-scaled size and high surface activity.

Monodispersed spherical TiO_2 particles have been researched extensively,[2–6] because an unagglomerated spherical particle with a narrow size distribution is the most desirable state for the compacting and sintering of ceramics. In the present study, micrometer-scaled, monodispersed and spherical TiO_2 particles with primary nanocrystallites are applied to improve the handling difficulty of the TiO_2 nanocatalyst. The spherical TiO_2 particles are expected to be easily manageable due to their micrometer-scaled size and to show sufficient photon efficiency due to their primary nanocrystallites.

Particle size is generally one of the most important physical parameters in a catalyst, because it can directly affect the number of active sites. There have been some systematic reports on the effects of particle size on TiO_2 photocatalysis.[7–17] The reported results can be summarized by the following three conflicting observations: the first is that photocatalytic activity decreased as particle size increased,[7] the second is that photocatalytic activity increased as particle size increased,[8–13] and the third is that maximum photocatalytic activity was shown in particles with diameters of about 10 nm.[14–17] The conflict among these three findings stems from the applications of photocatalysts prepared by different synthesis routes. Therefore, investigation of the influence of synthesis routes on photocatalytic activity is important in understanding the effects of particle size.

In the present study, monodispersed spherical TiO_2 particles with primary nanocrystallites were prepared by three different crystallization routes: (i) hydrothermal crystallization, (ii) calcination, and (iii) a combination of hydrothermal crystallization and calcination. The different crystallization routes provided TiO_2 particles with wide particle characteristics. Their photocatalytic activity was evaluated to elucidate the effect of the crystallization routes on the photocatalytic activity. Finally, it will be suggested that the hydrothermally crystallized particles should show ultrahigh photocatalytic activity due to their high surface adsorption ability for hydroxyl ions.

II. Experimental Procedure

(1) Synthesis and Crystallization of TiO_2 Particles

Amorphous spherical TiO_2 particles were synthesized by the thermal hydrolysis and condensation reactions of $TiCl_4$ in a mixed solvent of 1-PrOH and H_2O. In the mixed solvent, the volume ratio of 1-PrOH to H_2O was 3 and the concentration of HPC, a steric dispersant, was 0.3 g/L. $TiCl_4$ was dissolved in the mixed solvent to form a 0.1*M* $TiCl_4$ stock solution. The thermal hydrolysis and condensation reactions were induced by homogeneously heating 500 mL of the stock solution in a kitchen microwave oven. Detailed processing conditions and formation principles of the amorphous spherical precursor have been reported elsewhere.[6] In the present study, the amorphous TiO_2 precursor is referred to as AT particles, and it is used as a precursor for the subsequent hydrothermal and/or calcination processes.

The dried AT particles (1 g) were dispersed in 70 mL of H_2O by ultrasonic and stirring processes and then crystallized by hydrothermal process in a 100-mL Teflon-lined mini-autoclave. The hydrothermally crystallized TiO_2 particles are referred to as HT particles in the present study. After the hydrothermal crystallization, the HT particles were dried at 100°C for 12 h.

Some of the prepared HT particles were used as precursors for the combined crystallization process. The HT particles (1 g) were put into a platinum crucible and then rapidly heated to the desired

T. M. Besmann—contributing editor

Manuscript No. 187647. Received June 12, 2001; approved February 3, 2003.
The authors deeply thank the Research Institute of Industrial Science and Technology (RIST) for the financial support of this work.
*Member, American Ceramic Society.

calcination temperature. The hydrothermally crystallized and then calcined TiO_2 particles are referred to as HCT particles in the present study. In addition to the HT particles, the AT particles were simply calcined to prepare crystalline TiO_2 particles. The only calcined TiO_2 particles are referred to as CT particles in the present study.

For comparison, Degussa P-25 TiO_2 nanoparticles, one of the representative commercial photocatalysts, were used as a reference photocatalyst and are referred to as P25 particles in the present study.

(2) Characterization of TiO_2 Particles

Particle morphology was characterized by electron microscopy (SEM and TEM). Specific surface area (A) and light transmission behavior were evaluated by BET and UV–vis–IR spectroscopy, respectively.

Crystalline phase, fraction of crystallization (X_c), and diameter of primary nanocrystallites were evaluated by X-ray diffraction (XRD) analysis. In the XRD analysis, scanning speed, sampling interval, and range of 2θ were 0.4°/min, 0.01°, and 23.5–29°, respectively.

X_c refers to the fraction of the crystalline anatase phase in the particle where amorphous and crystalline anatase phases are mixed up. In the present study, the fraction of crystallization was evaluated by using the relative integral intensity of the anatase (101) diffraction peak, because the integral intensity is directly proportional to the fraction of crystalline phase. This evaluation method has been used to study the crystallization and phase transformation in TiO_2 particles under hydrothermal conditions.[18]

As will be further explained later, the prepared spherical particles were secondary agglomerates of primary nanocrystallites. The average diameter of primary nanocrystallite was calculated with the Scherrer formula from the peak broadening width at a half-intensity of the anatase (101) diffraction peak and was calibrated by the Warren method.[19] It is generally accepted that this method could be applied to measure the diameter of nanocrystallites smaller than 100 nm.[19] In the present study, the calculated diameter of primary nanocrystallites was compared with the results from TEM analysis. As the diameter of primary nanocrystallites becomes larger and larger, the mismatch of the XRD results to the TEM results becomes increasingly larger. Nevertheless, the deviation between the two results could be ignored in most of the prepared particles, except the HT particles crystallized under severe hydrothermal conditions.

In the XRD analysis to evaluate the fraction of crystallization and the size of primary nanocrystallites, commercial anatase particles (99.9%, Aldrich Chemical, Milwaukee, WI) with an average particle diameter of 200 nm were used as a reference sample.

Zeta-potentials were evaluated to investigate the surface adsorption ability for hydroxyl ions of the prepared TiO_2 particles suspended in aqueous solutions. In the zeta-potential analysis, various HCl and NH_3 aqueous solutions with different concentrations were used to control the pH of the TiO_2 suspensions.

(3) Measurement of Photocatalytic Activity

Photocatalytic activity was measured by monitoring chlorine ions generated during photocatalysis of chloroform ($CHCl_3$), a representative chlorinated hydrocarbon. A schematic illustration of the photocatalytic activity measurement system applied in the present study is presented in Fig. 1. For a prepared particle, the measured photocatalytic activity has narrow error limits, less than ±5%.

Photocatalysis of chloroform has been extensively studied.[20–22] Pruden and Ollis[20] suggested that chloroform should be readily degraded in illuminated TiO_2 suspensions according to the following reaction:

$$2CHCl_3 + 2H_2O + O_2 \xrightarrow{h\nu} 2CO_2 + 6HCl \quad (1)$$

As there is no intermediate product in reaction (1), the concentration of generated chlorine ions can be directly converted to the concentration of chloroform decomposed on the photocatalysis reaction. Therefore, in studies about the photocatalysis of chloroform, photocatalytic activity (γ) is generally defined as in the following equation:

$$\gamma = \frac{C}{3tmI} \quad (2)$$

where C is the concentration of chlorine ions (mol/L), t is the irradiation time of UV light, m is the concentration of TiO_2 particles (g/L), and I is the intensity of adsorbed UV light. In all the photocatalytic activity measurement tests, the initial concentration of chloroform and the added amount of the TiO_2 photocatalysts (m) were constant, being 0.019 mol/L and 0.62 g/L, respectively. In the present study, C was evaluated by using a chlorine ion selective electrode (96-17B, Orion Research, Inc., Beverly, MA), when the UV light irradiation time (t) was 20 min. As a UV light source, a UV black light lamp (15 W; F15T8/BLB, GE, Columbus, OH) was used and irradiated photons could not directly decompose chloroform without the aid of TiO_2 photocatalysts.

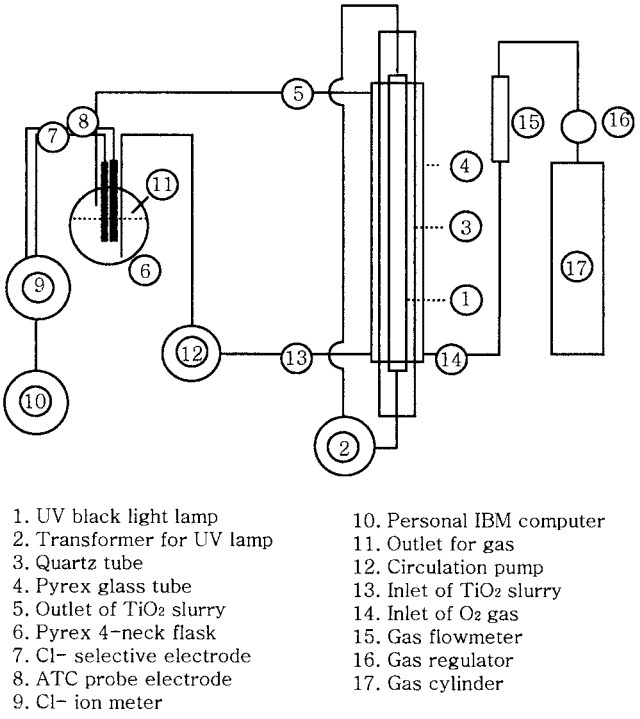

Fig. 1. Schematic view of the photocatalytic activity measurement system used in this study.

As represented in Eq. (2), the UV light transmission must be considered in calculating photocatalytic activity. In the present study, the transmission was excluded in the calculation process of photocatalytic activity ($I = 1$), because all the prepared particles showed the same UV light transmission behavior. Therefore, in the present study, photocatalytic activity (γ_1) is defined as in the following equation:

$$\gamma_1 = \frac{C}{3tm} \quad (3)$$

The photocatalytic activity (γ_1) calculated in Eq. (3) is an issue of practical importance and is defined as "volume activity" in the present study. From the viewpoint of materials science and chemistry, it is necessary that the activity be evaluated in terms of the amount of chloroform decomposed per unit area of crystalline anatase TiO_2 particles, because the volume activity depends on the number of active sites. The number of active sites is directly proportional to the fraction of crystallization and specific surface

area. In the present study, the photocatalytic activity normalized to the fraction of crystallization and specific surface area (γ_2) is defined as "chemical activity" and is represented in the following equation:

$$\gamma_2 = \frac{\gamma_1}{AX_c} = \frac{C}{3tmAX_c} \quad (4)$$

where A is the specific surface area measured by BET analysis and X_c is the fraction of crystallization evaluated by XRD analysis.

III. Results

(1) Synthesis and Materials Characteristics

SEM images of HT particles and P25 nanoparticles are presented in Figs. 2(a) and (b), respectively. The spherical particles shown in Fig. 2(a) were prepared by hydrothermal crystallization of AT particles at 200°C for 4 h. All the prepared spherical particles were 1 μm in diameter, monodispersed and spherical. From XRD analysis, all the prepared spherical particles were pure anatase, with the exception of the HCT and CT particles calcined at high temperatures and the P25 particles. The P25 particles were a mixture of anatase and rutile phases and composed of 86% anatase (22 nm) and 14% rutile (33 nm) particles. In the parentheses, XRD results for the diameters of anatase and rutile nanoparticles are presented. From the BET analysis, the specific surface area of the P25 particles was 42 m^2/g.

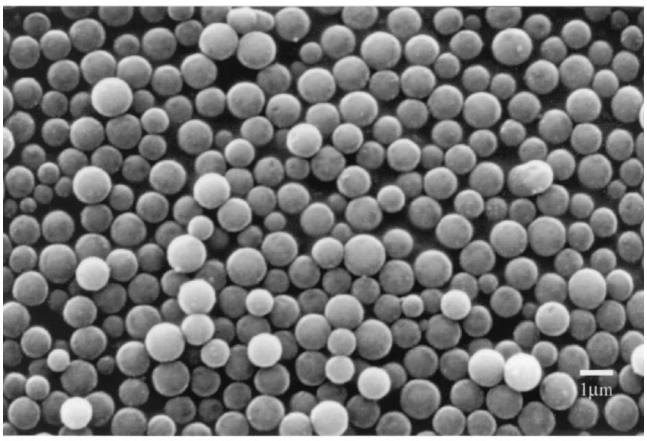

(a)

(b)

Fig. 2. SEM photographs of (a) prepared spherical particles and (b) the commercial P25 nanoparticles. The prepared particles were synthesized by hydrothermal crystallization of the AT particles at 200°C for 4 h.

In Figs. 3(a) to (h), TEM bright field images of the (a) P25, (b) AT, (c) HT, (d) HT, (e) HCT, (f) HCT, (g) CT, and (h) CT particles are shown, respectively.

The surfaces of the AT particles were smooth, and there was no evidence for the existence of primary nanocrystallites in the interior parts. The HT particles shown in Figs. 3(c) and (d) were prepared by hydrothermal crystallization of the AT particles at 160° and 240°C for 8 h, respectively. In the hydrothermal process, primary nanocrystallites formed and grew in the interior of the AT particles. The diameter of the primary nanocrystallites was highly dependent on the hydrothermal conditions and could be controlled to be in the range of 5–30 nm. Before and after the hydrothermal process, there was no change of spherical morphology, so that the average diameter was sustained to be about 1 μm.

The HCT particles shown in Figs. 3(e) and (f) were prepared by calcination of HT particles at 700° and 900°C for 1 h, respectively. The precursor HT particles were prepared by hydrothermal crystallization of the AT particles at 140°C for 6 h. Like the HT particles, the HCT particles were composed of primary nanocrystallites. As the calcination temperature increased, the size of the primary nanocrystallites increased. In the HCT particles, the diameter of primary nanocrystallites was controlled to be in the range of 5–50 nm by changing calcination conditions. Unlike the HT particles, the size of the spherical HCT particles decreased as the calcination temperature increased. The CT particles shown in Figs. 3(g) and (h) were prepared by simple calcination of the AT particles at 400° and 800°C for 1 h, respectively. The CT particles were spherical agglomerates of primary nanocrystallites. Like the HCT particles, as the calcination temperature increased, the diameter of primary nanocrystallites increased, whereas the diameter of the spherical particles decreased.

From TEM analyses, the following things are known: (i) All the prepared spherical particles were secondary agglomerates of primary nanocrystallites. (ii) The hydrothermal treatment resulted in the increment of the primary nanocrystallite size without changing the secondary particle size. On the other hand, the calcination process increased the primary nanocrystallite size and simultaneously decreased the secondary particle size. (iii) The diameter of primary nanocrystallites was controlled to be from a few nanometers to about 50 nm by changing crystallization routes and conditions.

In Table I, detailed synthesis conditions and materials characteristics (crystalline phase, fraction of crystallization, diameter of primary nanocrystallite, specific surface area, and light transmission) of some TiO_2 particles are presented. As the crystallization temperature and time increased, the fraction of crystallization and the size of the primary nanocrystallites increased, whereas the specific surface area decreased. The AT particles had a large specific surface area (366 m^2/g). On the other hand, the CT particles calcined at 800°C for 1 h had a very small specific surface area (5 m^2/g), even though the size of the primary nanocrystallites was so small (27 nm in diameter). The large specific surface area of the AT particles and the low specific surface area of the CT particles originated in the primary nanogels and the partial sintering between primary nanocrystallites, respectively. The partial sintering between primary nanocrystallites introduced considerable shrinkage to the spherical particles so that the size of secondary spherical particles decreased during the calcination processes.

Light transmission behavior of TiO_2 suspensions is closely related to the photocatalytic ability of a photocatalysis system as shown in Eq. (2). In Table I, the light transmissions of the TiO_2 suspensions for two kinds of light with wavelengths of 400 and 700 nm are included. All the aqueous TiO_2 suspensions prepared from the spherical TiO_2 particles showed the same light transmission behavior, even though each TiO_2 particle was prepared by different crystallization routes and had different sizes of primary nanocrystallites. The same light transmission behavior arose from the fact that the size of the spherical TiO_2 particles was nearly the same (about 1 μm in diameter). On the other hand, the P25 suspension showed different light transmission behavior from the spherical particles. The light transmission of the P25 suspension

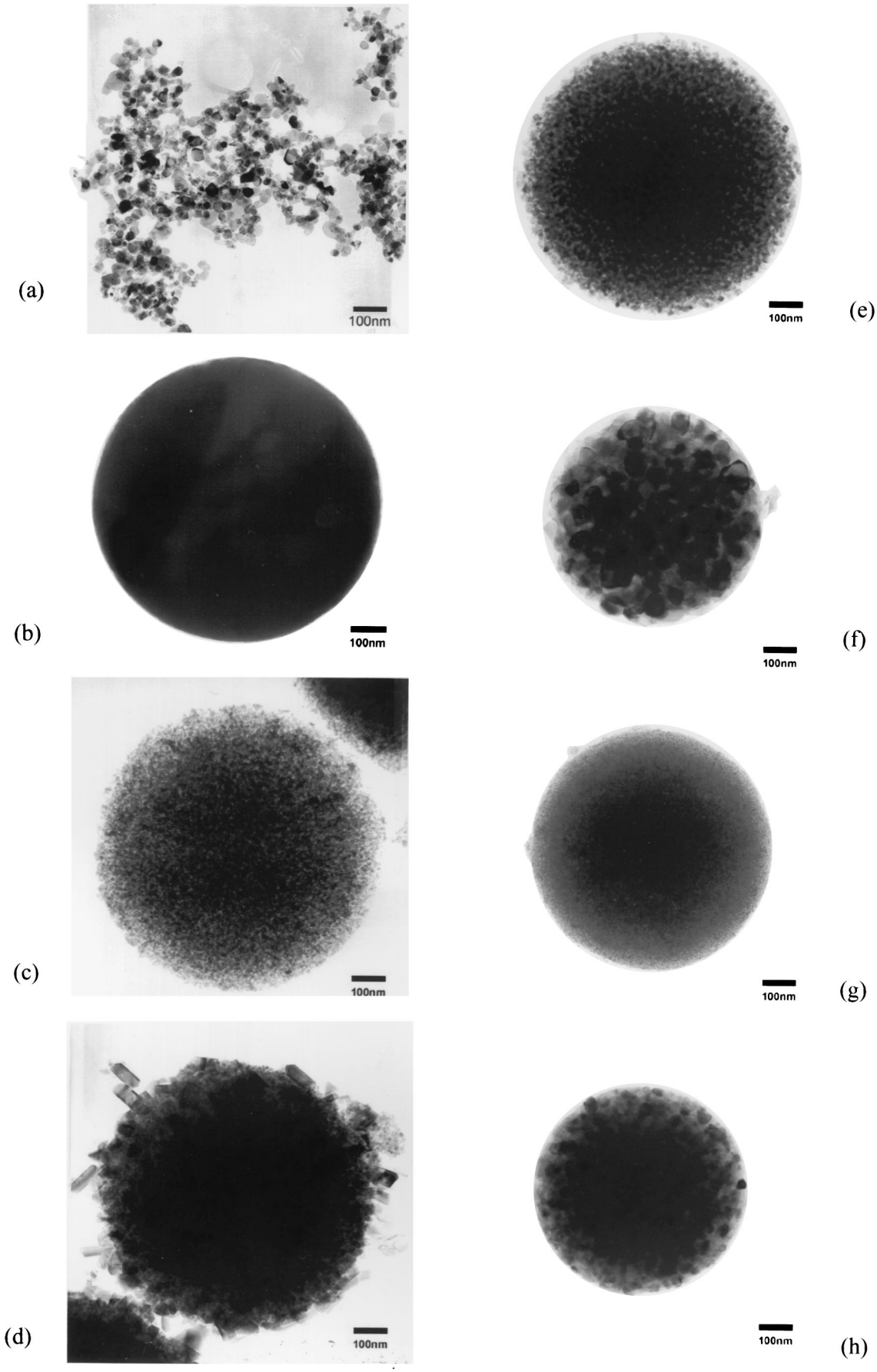

Fig. 3. TEM bright field images of (a) P25, (b) AT, (c) HT, (d) HT, (e) HCT, (f) HCT, (g) CT, and (h) CT particles. The HT particles in (c) and (d) were prepared by hydrothermal crystallization of the AT particles at 160° and 240°C for 8 h; the HCT particles in (e) and (f) were prepared by calcination of HT particles, hydrothermally crystallized at 140°C for 6 h and at 700° and 900°C for 1 h; and the CT particles in (g) and (h) were prepared by calcining the AT particles at 400° and 800°C for 1 h.

Table I. Detailed Synthesis Conditions and Some Materials Characteristics of the Prepared TiO_2 Particles

	Synthesis conditions		Materials characteristics					
							Light transmission†† (%)	
Samples	Hydrothermal process (°C/h)	Calcination process (°C/h)	Crystalline phase†,‡	X_c†,§	Diameter of primary nanocrystallite†,‡ (nm)	A¶ (m^2/g)	400 nm	700 nm
AT	—	—	A	0.14	3	366	0.08	0.06
HT	160/4			0.77	7	232	0.07	0.06
	240/4		A	0.76	9	123	0.07	0.06
	240/8	—	A	0.85	12	80	0.08	0.07
	240/32		A	0.81	26	31	0.07	0.06
	240/64			0.81	31	25	0.07	0.07
HCT	140/6	200/1	A	0.87	7	185	0.06	0.08
	120/6	600/1	A	0.81	7	159	0.07	0.07
	200/6	700/1	A	0.99	10	104	0.08	0.06
	200/6	800/1	A	1.07	17	52	0.07	0.07
	140/6	900/1	A	1.02	47	14	0.06	0.07
CT		300/1	A	0.26	4	288	0.07	0.08
		400/1	A	0.71	6	218	0.07	0.06
	—	600/1	A	0.88	9	125	0.08	0.07
		700/1	A	0.93	13	72	0.06	0.07
		800/1	A	0.95	27	5	0.07	0.06
P25	—	—	A (86%) R (14%)	0.98	22 (A) 33 (R)	42	0.02	0.25

†Evaluated by XRD analysis. ‡A and R refer to anatase and rutile, respectively. §X_c = fraction of crystallization. ¶A = specific surface area. Evaluated by BET analysis. ††Evaluated by UV–vis–IR analysis.

gradually decreased as the wavelength of irradiated light decreased. It is remarkable that the light transmission of the P25 suspension under the light with 400 nm in wavelength is similar to that of the spherical particle. All the TiO_2 suspensions showed sharp absorption behavior for UV light with a wavelength of 380 nm. This sharp absorption behavior resulted from the direct transition of valence electrons to the conduction band in anatase TiO_2.

(2) Photocatalytic Activity

UV light transmission must be considered to calculate photocatalytic activity as presented in Eq. (2). In the present study, the transmission was excluded in the photocatalytic activity calculation process ($I = 1$), because all the prepared particles showed the same UV light transmission behavior.

The volume activity (γ_1) of the HT particles as a function of hydrothermal time at each hydrothermal temperature is presented in Fig. 4. In the HT particles prepared at 120°C, the volume activity gradually increased and then decreased as the hydrothermal time increased. In the HT particles prepared at 160° and 200°C, the volume activity decreased as the hydrothermal time increased. In the HT particles prepared at 240°C, the volume activity decreased and then increased as the hydrothermal time increased. In the HT particles, the volume photocatalytic activity was very dependent on the hydrothermal temperature and time and was larger than that of the commercial P25 particles.

The volume activity (γ_1) of the HCT and CT particles as a function of calcination temperature is presented in Fig. 5. The HCT particles were prepared by calcining two kinds of HT particles, which were synthesized by hydrothermal crystallization of the AT particles at 140° and 200°C for 6 h, respectively. In the HCT particles, the volume activity rapidly decreased at low temperature (less than 400°C), increased at intermediate temperature (400–800°C), and then decreased at high temperature (more than 800°C), as the calcination temperature increased. On the other hand, in the CT particles, the volume activity increased and then gradually decreased, as the calcination temperature increased. In the calcined HCT and CT particles, the volume activity was very dependent on the calcination temperature and was much smaller than that of the commercial P25 particles, except for the HCT particles prepared by the calcination process at low temperatures.

IV. Discussion

(1) Importance of Crystallization Routes

From Figs. 4 and 5, it is obvious that the volume activity of TiO_2 particles is highly dependent on their own crystallization routes and conditions. The volume activities shown in Figs. 4 and 5 were replotted as a function of the diameter of primary nanocrystallites, one of the most important parameters in TiO_2 photocatalysis.[7–17] Figure 6 shows the variation of volume activity as a function of the diameter of primary nanocrystallites for the (□) HT, (△) HCT, (○) CT, and (▲) P25 particles. It is evident that the spherical TiO_2 particles prepared by different crystallization routes showed so diverse volume activity at the same diameter of primary nanocrystallites. In the HT particles, the volume activity

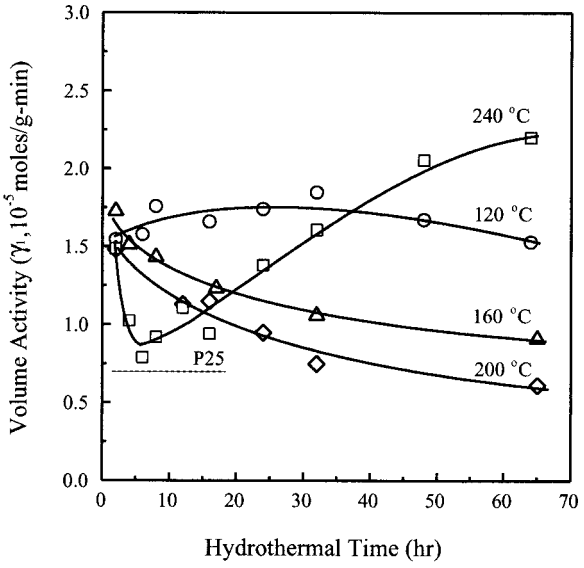

Fig. 4. Volume activity (γ_1) as a function of hydrothermal time for the HT particles prepared by hydrothermal crystallization at (○) 120°, (△) 160°, (◇) 200°, and (□) 240°C. The dotted line shows the photocatalytic activity of the commercial P25 particles.

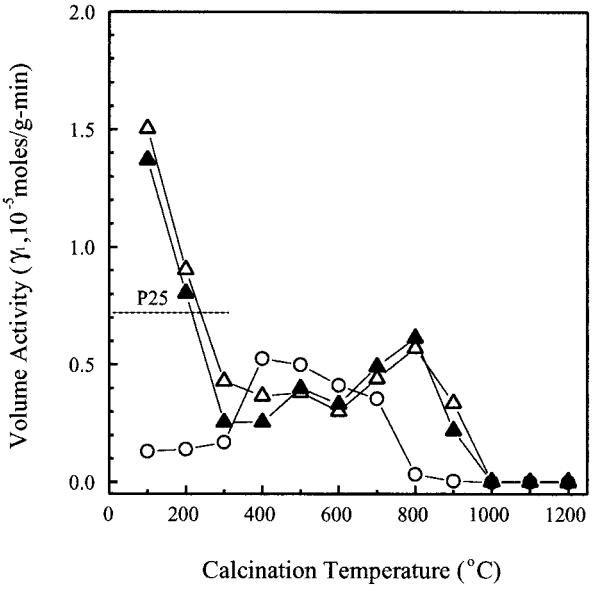

Fig. 5. Volume activity (γ_1) as a function of calcination temperature for the CT and HCT particles. The calcination time was 1 h; the precursors for calcination were the (○) AT and HT particles prepared by hydrothermal process at (△) 140° and (▲) 200°C for 6 h. The dotted line shows the volume activity of the commercial P25 particles.

decreased and then increased as the size of primary nanocrystallites increased. All the HT particles showed photocatalytic activity larger than the P25 particles. In the calcined HCT and CT particles, the photocatalytic activity increased and then decreased as the size of primary nanocrystallites increased. The calcined particles showed much smaller photocatalytic activity than the P25 particles.

The complex dependence behavior of volume activity on the size of the primary nanocrystallites could be simplified by a normalization process for both fraction of crystallization and specific surface area. Both fraction of crystallization and specific surface area are closely related to the number of active sites in TiO_2 photocatalysis. As the fraction of crystallization and specific surface area increase, the number of active sites increases, so that the volume photocatalytic activity increases. The normalized photocatalytic activity (chemical activity) is the photocatalytic activity per unit surface area of the crystalline anatase phase in a TiO_2 particle. In other words, the chemical activity is related to the intrinsic activity (of an active site) and the density of active sites (in unit surface area).

For the (□) HT, (△) HCT, (○) CT, and (▲) P25 particles, chemical activity (γ_2) as a function of the diameter of primary nanocrystallites is presented in Fig. 7. The chemical activity increased as the size of the nanocrystallites increased without concern for the crystallization route. The gradient of the chemical activity to the size of primary nanocrystallites was so dependent on the crystallization route. In the calcined CT and HCT particles, the slope was gentle, so that the chemical activity was nearly independent of the size of primary nanocrystallites. On the other hand, the slope of the HT particles was very steep, so that the chemical activity showed abruptly increasing behavior as the size of primary nanocrystallites increased. It is very interesting that the HT particles showed chemical activity superior to that of the calcined particles and appeared to have abruptly increasing chemical activity as the size of primary nanocrystallites increased.

(2) High Photocatalytic Activity of the HT Particles

The HT particles with large nanocrystallites had ultrahigh photocatalytic activity, about 3 times that of the P25 nanoparticles, even though they were secondary agglomerates of primary nanocrystallites. This means that the primary nanocrystallites in the interior part of the spherical HT particles actively participate in the photocatalysis reaction. Also, it implies that the chemical surface state, which is related to the intrinsic activity (of an active site) and density of active sites, might be the most important factor in the HT-particle-applied photocatalysis.

Zeta-potentials of some prepared TiO_2 particles as a function of pH are presented in Fig. 8. In parentheses, the diameters of the primary nanocrystallites are presented. It is remarkable that the HT particles have smaller isoelectric points (IEP) than the calcined HCT and commercial P25 particles. IEP is defined as the pH value at which the zeta-potential is zero and is related to the surface adsorption ability for hydroxyl ions. As the IEP value becomes smaller, the surface adsorption ability for hydroxyl ions becomes increasingly larger. Considering that the photocatalytic activity is directly proportional to the surface adsorption ability for hydroxyl

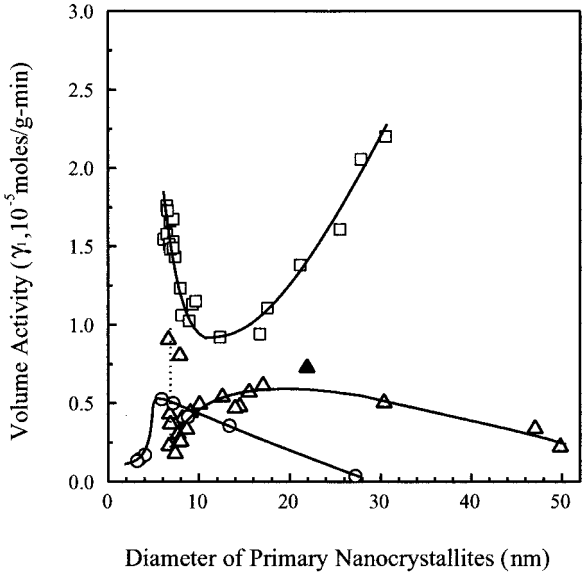

Fig. 6. Volume activity (γ_1) of the (□) HT, (△) HCT, (○) CT, and (▲) P25 TiO_2 particles as a function of the diameter of primary nanocrystallites.

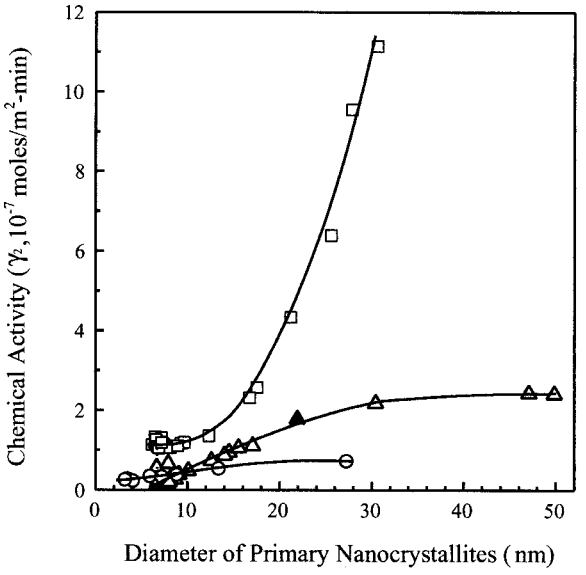

Fig. 7. Chemical activity (γ_2) of the (□) HT, (△) HCT, (○) CT, and (▲) P25 TiO_2 particles as a function of the diameter of primary nanocrystallites. The chemical activity was calculated by normalization of the volume activity (γ_1) to both fraction of crystallization (X_c) and specific surface area (A).

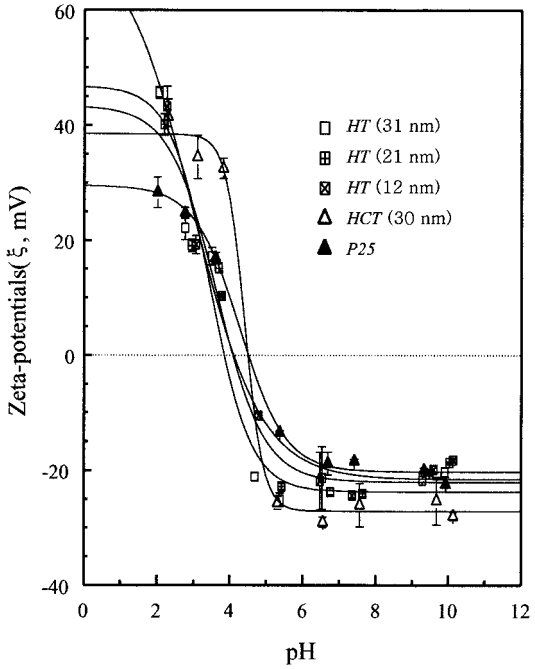

Fig. 8. Zeta-potential of HT, HCT, and P25 TiO_2 particles as a function of pH. The diameters of primary nanocrystallites of the HT and HCT particles are presented in parentheses.

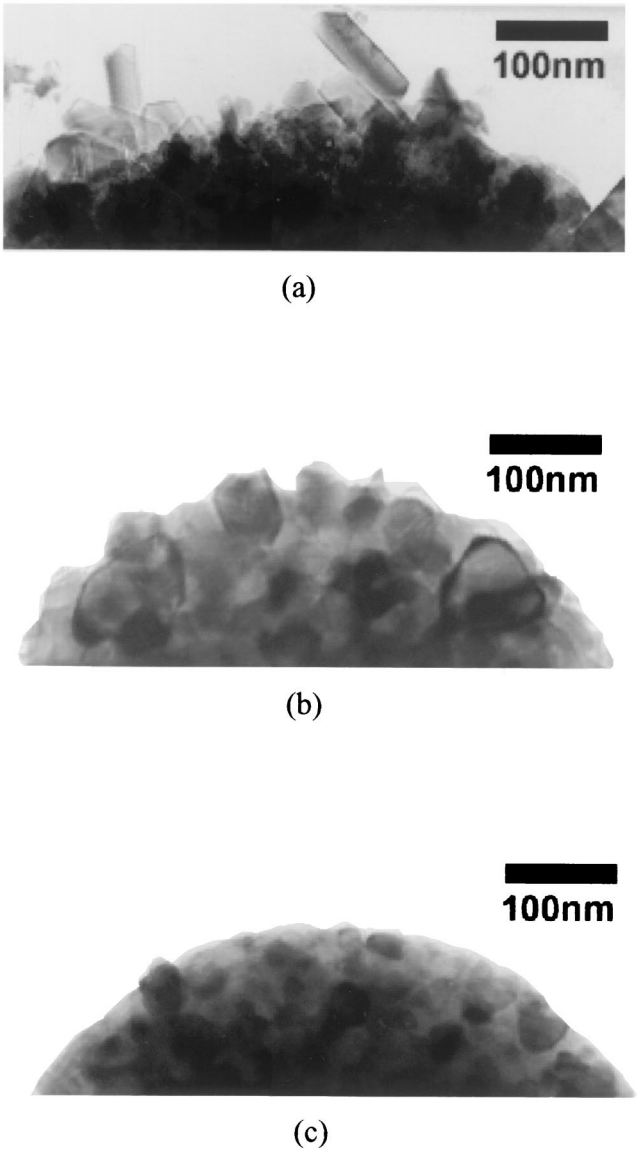

Fig. 9. TEM bright field images for the surface regions of (a) HT, (b) HCT, and (c) CT TiO_2 particles. The HT particles were hydrothermally crystallized at 240°C for 8 h, the HCT particles were prepared by calcining the HT particles (after hydrothermal crystallization at 140°C for 6 h) at 900°C for 1 h, and the CT particles were prepared by simple calcination of the AT particles (amorphous precursor) at 800°C for 1 h.

ions, it is evident that the difference in chemical activity between the HT and calcined particles originated from the difference between their chemical surface states, and the high volume activity of the HT particles with large nanocrystallites resulted mainly from their chemical surface state favorable to the photocatalysis (the high surface adsorption ability for hydroxyl ions).

It is well-known that hydrothermal processes produce well-developed defect-free single crystals.[23] TEM bright field images for the surface regions of representative HT, HCT, and CT particles are presented in Figs. 9(a) to (c), respectively. The primary nanocrystallites in the HT particles were so flat and faceted. On the other hand, the primary nanocrystallites in the calcined CT and HCT particles were rounded and more spherical. Therefore, in the present study, it appears that the high surface adsorption ability for hydroxyl ions of the HT particles is closely related to their well-developed nanocrystallite morphology.

One of the interesting findings in the present study was that the chemical activity of the HT particles increased as the size of primary nanocrystallites increased. Because the HT particles were composed of defect-free nanocrystallites and synthesized by the same crystallization routes, there was not much possibility that the intrinsic activity of the HT particles would increase as hydrothermal conditions were strengthened. Therefore, the strong dependency of photocatalytic activity on particle size could be suggested to originate in the increment of the density of active sites that was related to the preferential development of surface planes, easy to adopt hydroxyl ions.

V. Conclusions

The photocatalytic activity of monodispersed spherical TiO_2 particles with primary nanocrystallites showed complex dependence on their own crystallization route. The hyrothermally crystallized particles had superior photocatalytic activity to the calcined particles and appeared to have abruptly increasing photocatalytic activity as the size of primary nanocrystallites increased. The high photocatalytic activity of hydrothermally crystallized particles mainly resulted from their chemical surface state favorable to the photocatalysis (high surface adsorption ability for hydroxyl ions). The high surface adsorption ability for hydroxyl ions was closely related to the well-developed morphology of primary nanocrystallites. Also, the strong dependency of photocatalytic activity on particle size in the hydrothermally crystallized particles appeared to stem mainly from the preferential development of surface planes, easy to adopt hydroxyl ions. Therefore, in the present study, it was concluded that the particle morphology was one of the most important factors in the TiO_2 photocatalysis.

References

[1]Y. Fujishima and K. Honda, "Electrochemical Photolysis of Water at a Semiconductor Electrode," *Nature (London)*, **238**, 37–38 (1972).

[2]Y. Oguri, R. E. Riman, and H. K. Bowen, "Processing of Anatase Prepared from Hydrothermally Treated Alkoxy-Derived Hydrous Titania," *J. Mater. Sci.*, **23**, 2897–904 (1988).

[3]J. L. Look and C. F. Zukoski, "Alkoxide-Derived Titania Particles: Use of Electrolytes To Control Size and Agglomeration Levels," *J. Am. Ceram. Soc.*, **75** [6] 1587–95 (1992).

[4]M. Kondo, K. Shinozaki, R. Ooki, and N. Mizutani, "Crystallization Behavior and Microstructure of Hydrothermally Treated Monodispersed Titanium Dioxide Particles," *J. Ceram. Soc. Jpn.*, **102** [8] 742–46 (1994).

[5]H. K. Park, Y. T. Moon, D. K. Kim, and C. H. Kim, "Formation of Monodisperse Spherical TiO_2 Powders by Thermal Hydrolysis of $Ti(SO_4)_2$," *J. Am. Ceram. Soc.*, **79** [10] 2727–32 (1996).

[6]H. K. Park, D. K. Kim, and C. H. Kim, "Effect of Solvent on Titania Particle Formation and Morphology in Thermal Hydrolysis of $TiCl_4$," *J. Am. Ceram. Soc.*, **80** [3] 743–49 (1997).

[7]M. Anpo, T. Shima, S. Kodama, and Y. Kubokawa, "Photocatalytic Hydrogenation of CH_3CCH with H_2O on Small-Particle TiO_2: Size Quantization Effects and Reaction Intermediates," *J. Phys. Chem.*, **91**, 4305–10 (1987).

[8]K. Tanaka, M. F. V. Capule, and T. Hisanaga, "Effect of Crystallinity of TiO_2 on Its Photo-catalytic Action," *Chem. Phys. Lett.*, **187** [12] 73–76 (1991).

[9]A. Mills and S. Morris, "Photomineralization of 4-Chlorophenol Sensitized by Titanium Dioxide: A Study of the Effect of Annealing the Photocatalyst at Different Temperatures," *J. Photochem. Photobiol., A*, **71** [3] 285–89 (1993).

[10]J. F. Porter, Y. G. Li, and C. K. Chan, "The Effect of Calcinations on the Microstructural Characteristics and Photoreactivity of Degussa P-25 TiO_2," *J. Mater. Sci.*, **34** [7] 1523–31 (1999).

[11]C. K. Chan, J. F. Porter, Y. G. Li, W. Guo, and C. M. Chan, "Effects of Calcinations on the Microstructures and Photocatalytic Properties of Nanosized Titanium Dioxide Powders Prepared by Vapor Hydrolysis," *J. Am. Ceram. Soc.*, **82** [3] 566–72 (1999).

[12]S. Ito, S. Inoue, H. Kawada, M. Hara, M. Iwasaki, and H. Tada, "Low-Temperature Synthesis of Nanometer-Sized Crystalline TiO_2 Particles and Their Photoinduced Decomposition of Formic Acid," *J. Colloid Interface Sci.*, **216** [1] 59–64 (1999).

[13]Q. H. Zhang, L. Gao, and J. K. Guo, "Effects of Calcinations on the Photocatalytic Properties of Nanosized TiO_2 Powders Prepared by $TiCl_4$ Hydrolysis," *Appl. Catal., B*, **26** [3] 207–15 (2000).

[14]N. Serpone, D. Lawless, and R. J. Khairutdinov, "Size Effects on the Photophysical Properties of Colloidal Anatase TiO_2 Particles: Size Quantization or Direct Transitions in This Indirect Semiconductor?," *J. Phys. Chem.*, **99**, 16646–54 (1995).

[15]N. Serpone, D. Lawless, R. Khairutdinov, and E. Pelizzetti, "Subnanosecond Relaxation Dynamics in TiO_2 Colloidal Sols (Particle Sizes R_p = 1.0–13.4 nm). Relevance to Heterogeneous Photocatalysis," *J. Phys. Chem.*, **99**, 16655–61 (1995).

[16]C. Wang, Z. Zhang, and J. Y. Ying, "Photocatalytic Decomposition of Halogenated Organics over Nanocrystalline Titania," *Nanostruct. Mater.*, **9**, 583–86 (1997).

[17]Z. Zhang, C. Wang, R. Zakaria, and J. Y. Ying, "Role of Particle Size in Nanocrystalline TiO_2-Based Photocatalyst," *J. Phys. Chem. B*, **102**, 10871–78 (1998).

[18]K. Yanagisawa, Y. Yamamoto, Q. Feng, and N. Yamasaki, "Formation Mechanism of Fine Anatase Crystals from Amorphous Titania under Hydrothermal Conditions," *J. Mater. Res.*, **13** [4] 825–29 (1998).

[19]B. D. Cullity, *Elements of X-ray Diffraction*, 2nd ed.; p. 102. Addison-Wesley Publishing Co., Inc., Reading, MA, 1978.

[20]A. L. Pruden and D. F. Ollis, "Degradation of Chloroform by Photoassisted Heterogeneous Catalysis in Dilute Aqueous Suspension of Titanium Dioxide," *Environ. Sci. Technol.*, **17**, 628–31 (1983).

[21]C. Y. Hsiao, C. L. Lee, and D. F. Ollis, "Heterogeneous Photocatalysis: Degradation of Dilute Solutions of Dichloromethane (CH_2Cl_2), Chloroform ($CHCl_3$), and Carbon Tetrachloride (CCl_4) with Illuminated TiO_2 Photocatalyst," *J. Catal.*, **82**, 418–23 (1983).

[22]C. Kormann, D. W. Bahnemann, and M. R. Hoffman, "Photolysis of Chloroform and Other Organic Molecules in Aqueous TiO_2 Suspensions," *Environ. Sci. Technol.*, **25**, 494–500 (1991).

[23]W. J. Dawson, "Hydrothermal Synthesis of Advanced Ceramic Powders," *Am. Ceram. Soc. Bull.*, **67** [10] 1673–78 (1988). □